



Supplement of

Role of sea ice, stratification, and near-inertial oscillations in shaping the upper Siberian Arctic Ocean currents

Igor V. Polyakov et al.

Correspondence to: Igor V. Polyakov (ivpolyakov@alaska.edu)

The copyright of individual parts of the supplement might differ from the article licence.

1	Supplementary materials to the article:
2	Role of sea ice, stratification, and near-inertial oscillations in
3	shaping the upper Siberian Arctic Ocean currents
4	
5	Igor V. Polyakov ¹ , Andrey V. Pnyushkov ² , Eddy C. Carmack ³ , Matthew Charette ⁴ ,
6	Kyoung-Ho Cho ⁵ , Steven Dykstra ⁶ , Jari Haapala ⁷ , Jinyoung Jung ⁵ , Lauren Kipp ⁸ , Eun
7	Jin Yang ⁵ , Sergey Molodtsov ²
8	
9	1 International Arctic Research Center and College of Natural Science and Mathematics, University of
10	Alaska Fairbanks, Fairbanks, 99775, USA
11	2 International Arctic Research Center, University of Alaska Fairbanks, Fairbanks, 99775, USA
12	3 Institute of Ocean Sciences, Fisheries and Oceans Canada, 9860 West Saanich Road, Sidney, BC, V8L 4B2, Canada
13	4 Woods Hole Oceanographic Institution, 266 Woods Hole Road, Woods Hole, Massachusetts, 02543, USA
14	5 Korea Polar Research Institute, Incheon, Korea
15	6 College of Fisheries and Ocean Sciences, University of Alaska Fairbanks, Fairbanks, USA
16	7 Finnish Meteorological Institute, Helsinki, Finland
17	8 Rowan University, 201 Mullica Hill Road, Glassboro, New Jersey, 08028, USA
18	
19	Correspondence to: Igor V. Polyakov, 907-474-2686, ivpolyakov@alaska.edu
20	
21	
22	
23	
24	
25	
26	

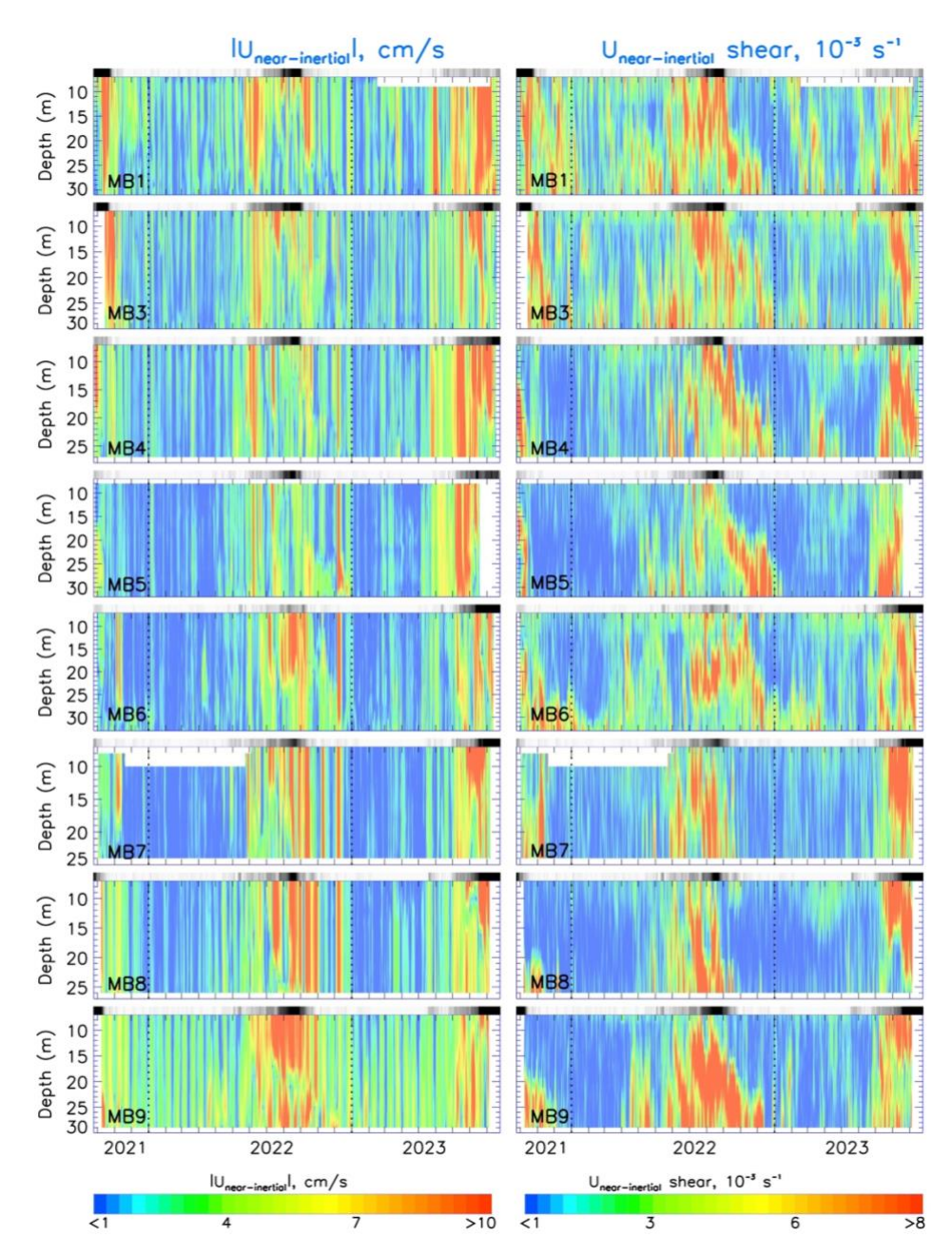


Figure S1: Biennial (September 2021– September 2023) records, showing the magnitude of the semidiurnal-band (near-inertial) currents (left) and associated shear (right) at eight NABOS mooring locations (see **Fig. 1**) as a function of time and depth. White segments show missing data. Black-greywhite bar over each panel shows daily sea ice concentration between 0% (black indicating ice-free summer) to 100% (white indicating winter), with near grey scale for interseasonal transitions. Vertical dotted lines show transitions from year to year. Note that there are minor variations in the vertical data coverage of the mooring records.

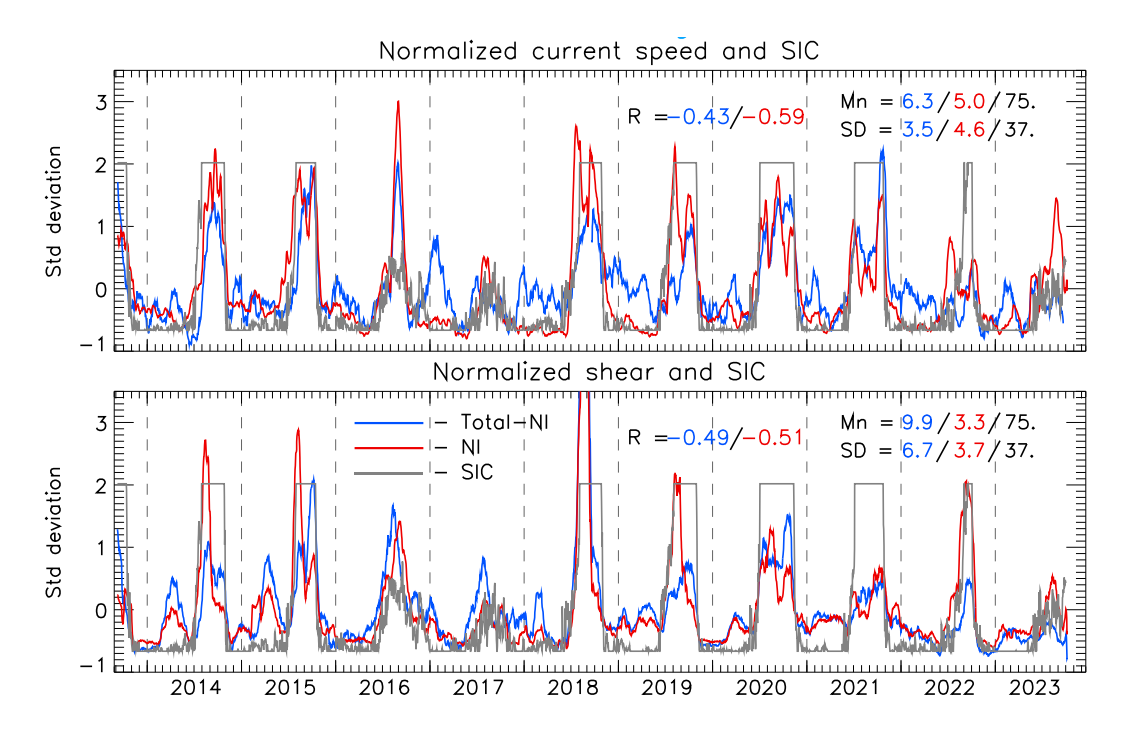


Figure S2: Time series of normalized (reduced to anomalies by subtracting means, Mn, and divided by standard deviations, SD) current speed $|\mathbf{U}|$, vertical shear of horizontal current $|\mathbf{U}_z|$ (both from 10m depth level), and sea ice concentration SIC (the latter time series are multiplied by minus one) at M1 mooring location. Blue lines show parameters for total minus near-inertial currents, red lines show parameters for near-inertial currents, and gray lines show SIC. Mn and SD are provided for $|\mathbf{U}|$ in cm/s, $|\mathbf{U}_z|$ in 10^3 s⁻¹ and SIC in %. Correlations *R* between $|\mathbf{U}|$ and SIC (blue digits) and $|\mathbf{U}_z|$ and SIC (red digits) are all statistically significant at 0.05% level.

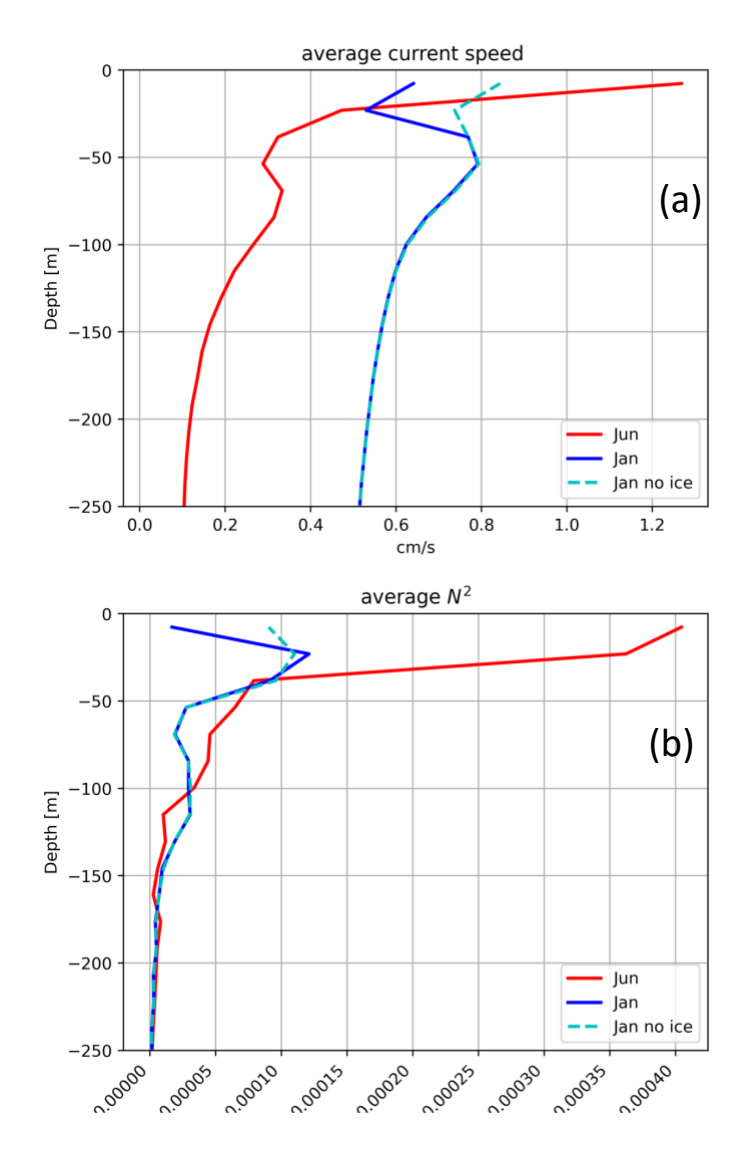


Figure S3: Vertical profiles of model-based, wind-forced current speed (a, cm s⁻¹) and squared buoyancy frequency (b, s⁻²) under summer and winter conditions. Additional profiles (blue dashed lines) represent results from the experiment in which sea ice was excluded from the model.